Available online at www.sciencedirect.com
ScienceDirect
Journal of Power Sources 160 (2006) 733–743
JOURNAL OF POWER SOURCES
www.elsevier.com/locate/jpowsour

Cationic substitution in γ-type nickel (oxi)hydroxides as a means to prevent self-discharge in Ni/Zn primary batteries

F. Bardé [a,*], M.R. Palacín [b], B. Beaudoin [a], P.A. Christian [c], J.-M. Tarascon [a]

[a] *Laboratoire de Réactivité et de Chimie des Solides, Université de Picardie Jules Verne, CNRS UMR 6007, 80039 Amiens, France*
[b] *Institut de Ciència de Materials de Barcelona, ICMAB-CSIC, Campus UAB, 08193 Bellaterra, Catalonia, Spain*
[c] *Gillette, Gillette Technical Center, 37 A Street, Needham, MA 02494-2806, United States*

Received 13 October 2005; accepted 21 December 2005
Available online 15 February 2006

Abstract

The self-discharge of γ-NiOOH in Ni/Zn primary batteries was studied on real cells and also on chemically simulated ones. The results indicate that it is rooted in a dissolution/re-crystallization process, probably involving an α-type nickel hydroxide intermediate. To minimize this phenomenon, the preparation of a series of diverse metal substituted γ-type nickel hydroxides was attempted by oxidation of α-type precursors containing various amounts of Al, Cd, Co, Cr, Fe or Zn, prepared by direct precipitation at room temperature in an ammonia containing reaction medium. These reactions led to metal substituted γ-type nickel oxihydroxides in all cases except for cadmium and chromium containing samples. For the former phase segregation took place whereas for the latter a complete dissolution of chromium species in the reaction medium was observed. Partial dissolution was found to take place also for aluminium substituted phases. High temperature storage tests conducted on Ni/Zn primary cells using the substituted γ-phases as the positive electrode indicate that iron and cobalt substitution is effective in preventing self-discharge phenomena observed in pure γ-NiOOH, as aged cells presented discharged capacities very similar to fresh cells.

Keywords: Substitution; Nickel (oxi)hydroxide; Self-discharge; Primary battery; Alkaline batteries

1. Introduction

Despite the emergence of Li-ion battery technology, the Ni-based system remains nowadays widely used especially with the appearance of Hybrid/Electric Vehicles or new portable devices demanding high power such as digital cameras. With respect to the use of nickel electrodes in rechargeable cells, most of the studies have been focused on improving their conductivity, capacity or cyclability (i.e. lifetime), but only a few have been dedicated to the self-discharge phenomenon of nickel oxihydroxides. Megahed and co-workers were the first to evidence that the self-discharge consisted of a reduction of NiOOH to yield $Ni(OH)_2$ and oxygen gas [1], and later on Sac-Epée et al. made a study on self-discharge specific to Ni/H_2 batteries [2–4]. Bode et al. [5] established the possible occurrence of four phases in the nickel electrode system, two in the reduced state: α-$Ni(OH)_2$ and β-$Ni(OH)_2$ (from now on denoted αII and βII) and two in the oxidized state γ-NiOOH and β-NiOOH (i.e. γIII and βIII). The structures of all of these phases consist of diverse stacking of layers of edge sharing NiO_6 octahedra. In the case of βII and βIII, only protons are present in the interlayer space whereas in γIII and αII water molecules and other species are also present leading to a dilated *c* parameter [6,7]. The γIII/αII couple is, in principle, more attractive than the βIII/βII one due to the fact that the γIII phase presents a higher oxidation state for nickel resulting in a higher theoretical number of electrons exchanged (i.e. 1.5 EE for γIII/αII against only 1 EE for the βIII/βII couple). Numerous studies have been aimed towards taking advantage of the large capacity associated to the γIII/αII couple, but numerous difficulties were encountered in solving the problematic bottleneck associated to the fact that the γIII/αII couple is relatively unstable in alkaline medium and rapidly evolves into the βIII/βII couple [8]. Among the methods used to avoid the γIII/αII evolution into βIII/βII upon cycling, the most common one has been to partially substitute the nickel atoms within the nickel hydroxide layers for other metals. Two main synthetic routes

* Corresponding author. Present address: Toyota Motor Europe, 21, avenue des Volontaires, 3 eme etage, 1160 Auderghem, Belgium.
Tel.: +32 2 712 88 03; fax: +32 2 712 31 69.
E-mail address: fanny.barde@u-picardie.fr (F. Bardé).

0378-7753/$ – see front matter © 2006 Elsevier B.V. All rights reserved.
doi:10.1016/j.jpowsour.2005.12.073

to substitute nickel hydroxide have been reported: the direct co-precipitation taking place in solution, and a "chimie douce" process involving the hydrolysis of samples prepared at high temperature. Using the first approach, samples have been prepared containing cobalt [9], aluminium [10], zinc [11–13], iron [14] or manganese [15,16] whereas the second allowed to obtain iron [17] or cobalt [14,18,19] substituted phases. On the other hand, chromium-substituted α-type nickel hydroxides have also been prepared by electrodeposition from a nickel nitrate solution containing chromate ions [20,21]. The effects of these cationic substitution are diverse: cobalt, aluminium or iron substitution completely stabilises the α-type phase inhibiting transformation to βII [9,10,14,18] but the latter two induce chargeability problems and a decrease in the effective capacity, respectively. The Zn substitution was shown to lead to a similar stabilizing effect, but upon aging in concentrated KOH electrolyte, a migration of zinc to the inter-layer space takes place, and the phase transformation to βII is observed [11–13,17]. Similarly, chromate formation and therefore dissolution are observed for chromium-substituted phases. [21] Finally, manganese substitution yields to the formation of interstratified phases [15,16].

The objective of the present work is roughly different from the above-mentioned research since it is first aimed at understanding the self-discharge mechanism of γ-NiOOH in Ni/Zn primary cells and second at testing the effect of cationic substitution in this phenomenon. Thus, the substitution is here aimed at decreasing the self-discharge phenomenon rather than stabilizing the γIII/αII couple against the βIII/βII one. Thus, despite the disheartening results reported in some cases, we revisited the preparation of aluminium-, cobalt-, iron-, cadmium-, zinc- and chromium-substituted α-type phases, and attempted to prepare the corresponding oxidized substituted γIII oxi-hydroxides in order to test the effect of cationic substitution on the self-discharge of these phases in real Ni/Zn primary batteries. To ease the comparison, all substituted α-II phases were prepared by the same direct precipitation method. Ammonia was chosen as alkaline precipitating agent as previously reported only for aluminium substituted samples [10], owing to its ability to complex metals and thus to avoid phase segregation. The oxidation of these samples to γ-III was carried out in alkaline aqueous medium using NaClO as oxidizing agent. To our knowledge, it is the first time that the substitution of γ-type phases synthesized in aqueous media is reported.

2. Experimental

Samples were characterized by means of XRD, SEM and EDXS. The phase composition was determined by X-ray powder diffraction using a Philips diffractometer PW1710 with Cu Kα radiation (λ = 1.54957 Å). Given the poor crystallinity of the studied phases, the X-ray patterns were registered within a 5–75° angular window, high acquisition time (10 s) and a step of 0.02°. Energy Dispersive X-ray Spectroscopy (EDXS), using a Philips XL-30FEG Scanning Electron Microscope (SEM), determined the amount of substituting element and also allowed confirming the homogeneity of the samples. The average oxidation state of the metal elements within the prepared phases was determined by iodometric titration, whereas the total amount of nickel was determined by titration with an ethylene diamine tetraacetic acid (EDTA) solution. Typically, 100 mg of the sample were added to 1.5 g of potassium iodide, and the mixture was dissolved in an acetic buffer solution. Sodium thiosulfate was used to titrate the iodine produced during nickel reduction. Then, a 28% ammonia solution was added to the medium and the complexometric titration was carried out with 0.1 M EDTA solution in the presence of murexide as indicator. The analyses were carried out twice on each sample. It should be noticed that only species such as Ni(III), Ni(IV) and Co(III) Co(IV) are titrated by this process, whereas Al(III), Fe(III) or Zn(II) do not participate in the titration reaction.

Electrochemical tests were performed in Ni/Zn cell primary button cells. The anode consisted of zinc slurry and the cathode was a mixture of NDG15-type industrial graphite and active material (i.e. the substituted γ-type nickel oxihydroxide to be tested) in a 20/80 ratio compacted up to 1 t cm^{-2} whereas the electrolyte used is 9N potassium hydroxide. Galvanostatic tests were carried out at room temperature on an Arbin cycler at C/20 discharge rate. The interest in using button cells is that the cells are sealed, preventing changes in the electrolyte (water loss and consequent potassium hydroxide crystallization) upon heating. In all cases, eight identical button cells containing the same M-substituted phase were built and four of them were immediately discharged while the remaining four were aged at 60 °C for 24 h in order to enhance self-discharge.

3. Results and discussion

3.1. Study of the self-discharge phenomenon

In order to ascertain the reaction pathway for the self-discharge of γ-NiOOH, we pursued a double and complementary approach: on one hand, we studied the mechanism in real operating conditions (i.e. in real Ni/Zn cells at high temperature) and on the other we performed a chemical simulation of these conditions in order to study "clean" samples (e.g., carbon- or Zn-free samples).

In the first case, button cells were assembled with the positive electrode containing a mixture of NDG15 carbon (60%) and γ-NiOOH (40%) issued of chemical oxidation of commercial β-Ni(OH)$_2$ using the already described oxidation reaction [22]. The negative electrode consisted of a mixture of Zn and ZnO whereas the electrolyte used was KOH 9 M. The cells were aged in an oven at 55 °C during 4 months, after which they were highly deformed, certainly due to the high internal pressures caused by the release of oxygen. The positive electrode active material was recovered and its XRD pattern (Fig. 1) indicated that it consisted of pure β-Ni(OH)$_2$ with carbon and also some ZnO accidentally mixed with the powders during the process of recovery. Thus, under these conditions the cells are fully self-discharged, as no signs of the pristine γ-NiOOH appear in the XRD pattern. The study of this electrode active material by SEM reveals that the sample contains a high number of hexagonal platelets (around 1000 Å in diameter) (Fig. 2), certainly corresponding to Ni(OH)$_2$. The changes in morphol-

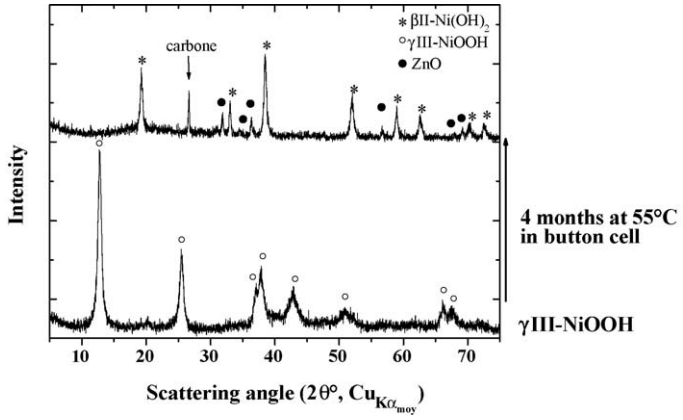

Fig. 1. X-ray diffraction patterns of the positive active material in fresh Ni/Zn cells (pristine γ-NiOOH) and cells aged for 4 months at 55 °C (carbon and ZnO from the negative electrode also appear).

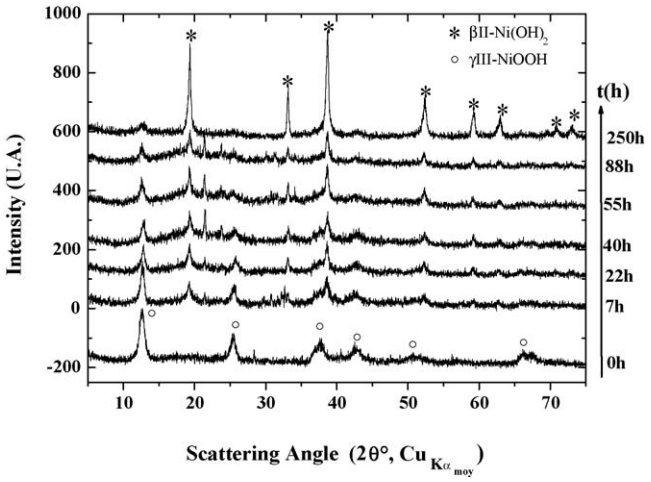

Fig. 3. X-ray diffraction patterns of the evolution of γ-NiOOH during aging in an autoclave at 115 °C under 4 bar oxygen pressure.

ogy during the self-discharge process are clear evidence that the γ(III) → β(II) phase transformation does not take place in the solid state as observed in less drastic conditions [23] but through a dissolution/re-crystallization process.

This was confirmed by "chemical simulation" of the self-discharge process. Two sets of experiments were carried out. The first one consists in the ageing of a γ-NiOOH in KOH 9M solution at 55 °C under stirring for 16 days, and the second one the ageing of the same solution in an autoclave, using more drastic conditions $T = 115$ °C and $P = 40$ bars oxygen pressure. In the first case, the XRD pattern of the final sample (Fig. 3) again indicates that the sample consists of pure β-$Ni(OH)_2$. During the second experiment, sample aliquots were taken as a function of time and X-ray diffraction patterns were taken once centrifuged. A gradual transformation from γ-NiOOH to β-$Ni(OH)_2$ was also observed. Transmission and scanning electron microscopy examinations indicate that both aged samples consist of monolithic hexagonal platelets (Fig. 4). The monolithic nature of the particles is a clear proof that the transformation goes through a dissolution/re-crystallization process that might involve the presence of an intermediate αII phase. Indeed, the instability of this phase in alkaline medium would be fully consistent with the dissolution/re-crystallization mechanism.

3.2. Synthesis and characterization of substituted α-type nickel hydroxides

The pure α-$Ni(OH)_2$ phase was synthesized according to Le Bihan's method [6], for which 500 mL of a 1 M nickel nitrate solution prepared from $Ni(NO_3)_2{\cdot}6H_2O$ were added to 65 mL of ammonia solution ($NH_4OH{\cdot}H_2O$, 28%) under strong stirring at room temperature. After 2 h of reaction time, the obtained green precipitate was copiously washed with water and acetone prior to being dried at room temperature in ambient atmosphere and characterized for its structural and textural properties. Substituted α-type nickel hydroxide was prepared following the same process but starting from a 1 M nitrate solution containing both nickel and the substituting metal (Al, Cd, Co, Cr, Fe, Zn). Samples are denoted M-x%(sol) where M is the substituting metal and x is its molar percent (i.e. $100 \times (n_M/n_{Ni})$) in the starting solution. When this solution was added to the concentrated ammonia, a precipitate instantaneously appeared. This precipitate was immediately recovered from the solution by centrifugation in order to avoid any eventual evolution of the αII-type phase to βII-type.

The X-ray diffraction patterns of the entire prepared samples are shown in Fig. 5. As expected, in all cases the major

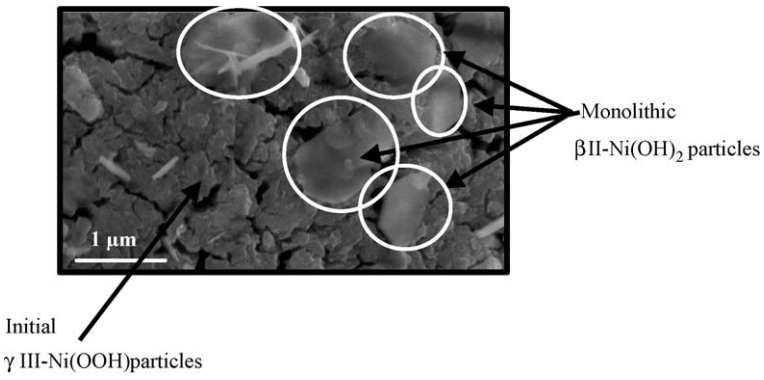

Fig. 2. Typical SEM image of the positive active material in Ni/Zn cells aged for 4 months at 55 °C exhibiting the presence of a large amount of well crystallised hexagonal platelets.

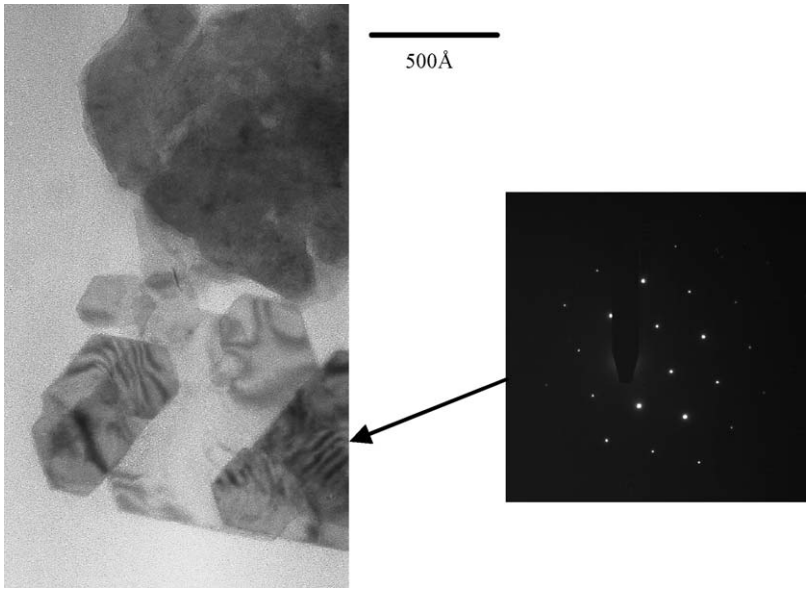

Fig. 4. TEM image and corresponding electron diffraction pattern of the hexagonal platelets present in the aged "γ-NiOOH". Both are typical of β-$Ni(OH)_2$ monolithic particles.

phase was the αII-type phase as deduced from XRD indexing according to the 22-0444 *JCPDS* file. In some cases, minor βII-type impurities (marked with an asterisk) were observed. With M = aluminium, a pure α-type phase was obtained for high substitution degrees [Al-20%(sol)] whereas for smaller ones, a shoulder attributed to the β-type phase appeared within the 0 0 2 peak of the αII phase. Furthermore, with increasing the degree of substitution we note a shift of the 0 0 1 diffraction peak to lower scattering angles indicating that the *c* lattice parameter evolves from 7.35 Å for Al-5%(sol) to 8.63 Å for Al-20%(sol). All zinc substituted samples contain essentially the αII-type phase but exhibit the 0 0 1 diffraction peak of the β-$Ni(OH)_2$ phase and an evolution of the *c* lattice parameter from 7.63 Å to 9.15 Å is observed for Zn-1%(sol) and Zn-5%(sol), respectively. β-$Ni(OH)_2$ impurities are also observed in all chromium substituted samples but more remarkably, a decrease in crystallinity is found to take place with increasing the chromium content. In this case, the *c* parameter varies between 7.49 Å for Cr-2.5%(sol) and 8.27 Å for Cr-20%(sol). A more enhanced amorphization phenomenon is induced by iron substitution but no β-$Ni(OH)_2$ impurities are observed. In this case, the *c* lattice parameter is found to evolve from 7.13 Å to 7.83 Å for Fe-2.5%(sol) and Fe-20%(sol), respectively. In contrast, the X-ray diffraction patterns of cadmium-substituted phases are characteristic of well-crystallized α-type phases and in this case the presence of β-$Ni(OH)_2$ is only detected for Cd-5%(sol). Finally, for cobalt-substituted hydroxides the X-ray diffraction patterns are again characteristic of the α-type phase and only the Co-15%(sol) contains β-$Ni(OH)_2$. Their *c* lattice parameters are 8.39 Å, 7.56 Å and 8.96 Å for Co-1%(sol), Co-5%(sol) and Co-15%(sol), respectively.

Overall, a common denominator to all the substituted phases is the increase in the *c* lattice parameter with the degree of substitution. The reasons for this are diverse. With M = Cd, this could be attributed to its larger ionic radius as compared to Ni [24]. On the other hand, for samples containing trivalent metals, with smaller ionic radius, a possible explanation to account for the large cell parameters obtained could consist in considering that when a trivalent element replaces bivalent nickel, the supplementary positive charge has to be compensated with the presence of a higher amount of anionic species between the layers. The case of zinc is particular; former studies by Tessier et al. [11–13] demonstrated that this element at the +II oxidized state is placed in the tetrahedral position available in the interlamellar space, inducing the additional intercalation of carbonates.

The percent of substituting metal within each sample was determined by Electron Dispersive X-ray Spectroscopy and its distribution homogeneity checked by SEM. As expected, the metal percent in the solid (denoted M-*x*%(α)) is not the same as compared to the initial solution (M-*x*%(sol)), indicative of the difficulties encountered in preparing desired stoichiometry samples by this low temperature precipitation route. The condensation of single cations in solution depends on multiple parameters (thermodynamic and kinetic) [25], and this scenario is even more complicated when different types of cations are precipitated simultaneously. From a thermodynamic point of view, the phases containing mixed cations are expected to be more stable, but from a kinetic point of view, if the precipitation rates of the mixed phase and the pure phases issued from the precipitation of each cation alone are of the same order, the reaction leads to phase segregation. In our study, no segregation of elements was observed but no prediction of the final substituting metal content could be made prior to carrying out the series of synthesis. The final substituting metal percent in the solid determined by EDXS (M-*x*%(α)) is plotted as a function of the ratio in the initial solution (M-*x*%(sol)) in Fig. 6. In all cases except for cadmium, the points fall above the diagonal of the plot, indicating that a higher ratio of substituting metal in the solid than in the mother solution is obtained, the highest difference being observed for cobalt. Even though as stated above, predictions

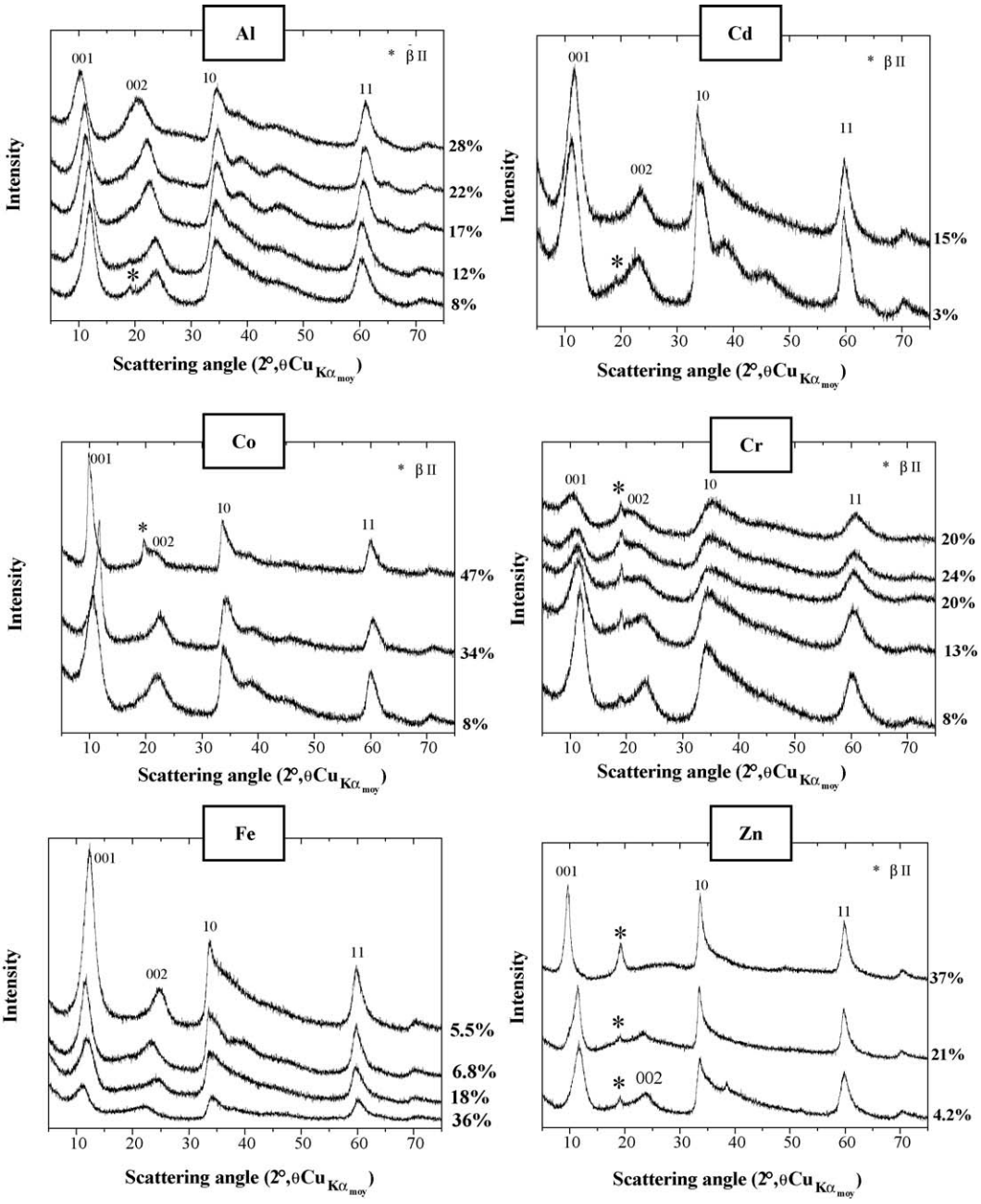

Fig. 5. X-ray diffraction patterns of M-substituted α-type nickel hydroxide denoted M-*x*%(α) (with M = Al, Cd, Co, Cr, Fe or Zn) reported as a function of the experimentally determined percentage of metal (*x*). βII phase impurities are marked with an asterisk.

of the final percent of substituting metal are not possible, it is worth pointing out that cadmium is the only substituting element forming a hydroxide with higher solubility than nickel hydroxide [26] whereas cobalt is the one forming the most insoluble hydroxide.

The most representative Scanning Electron Microscopy images corresponding to M-substituted α-type hydroxides have been selected for samples presenting similar substitution degrees and are depicted in Fig. 7 together with an image of pure α-$Ni(OH)_2$ hydroxide at the same scale. Pure nickel hydroxide is composed of aggregates with a 2 μm average diameter, that are themselves constituted of very thin tangled films (Fig. 7). In the cases of substitution with cobalt, cadmium or zinc elements, this airy texture is preserved whereas for samples containing aluminium, chromium or iron, the thin tangled films cannot be distinguished, and the sample seems to be more dense.

3.3. Chemical oxidation of substituted α-type phases

The substituted αII phases were chemically oxidized according to the previously reported protocol [22]. The reaction was performed in a water bath at 60 °C. 1.5 g of the substituted α-type precursor hydroxide were added to 200 mL of a concentrated potassium hydroxide solution (KOH 5N) and then 200 ml of 13% NaClO was added drop by drop and stirring was maintained for 4 h. The resulting products were centrifuged and washed several

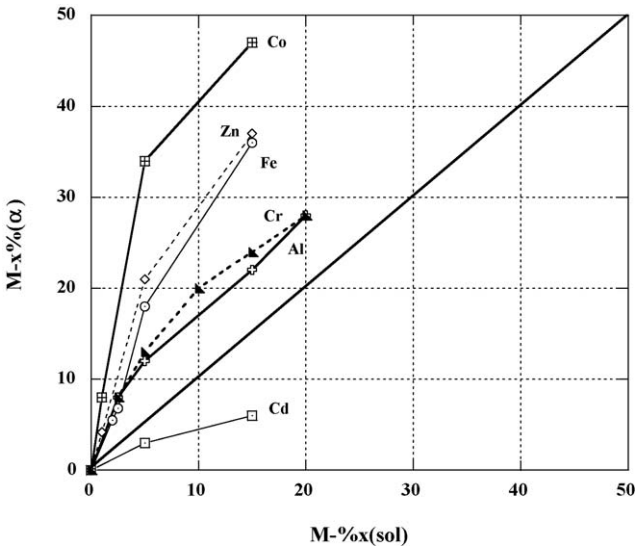

Fig. 6. Plot of the experimental percent of M recovered in M-substituted α-type precipitate determined by EDXS (denoted M-*x*%(α)) as a function of the percent of M present in the initial mother solution (denoted M-*x*%(sol)) with M = Al, Cd, Co, Cr, Fe or Zn. In all cases except for M = Cd, the amount of metal in the resulting α phase is higher than that present in the mother solution.

times until neutral pH was achieved, before being dried at 55 °C. For reasons of clarity, they are denoted in the following as M-*x*%(γ) where *x* is percent of substituting metal determined by EDXS. The X-ray diffraction patterns of the oxidized phases M-*x*%(γ), reported in Fig. 8 indicate that the samples are usually well crystallized with the γIII-type phase, as deduced from the XRD indexing according to the (06-0075 *JCPDS*) file, as the major phase. Occasionally, some of them contain traces of βIII-type oxihydroxide or a small amount of remaining αII-type precursor, indicating that the oxidation is not complete.

Under the reaction conditions listed above, we noted that when M = Al the oxidation is only completed for Al-8%(α) precursor. We further found that the final oxidized γIII-type phase resulting from such precursor only contains Al-3.5%(γ) of aluminium, indicative of the partial dissolution of aluminium during the oxidation process. In the case of iron-substituted phases, βIII impurities are observed and the percentages of iron within the samples issued from the oxidation of Fe-5%(α) and Fe-7%(α) were determined as Fe-5%(γ) and Fe-6%(γ), indicating that the amount of iron dissolution, if any, is very low. When M = Zn, the oxidation is almost complete in most cases (except for Zn-37%(γ) containing traces of αII) and no zinc dissolution is observed either. Finally, regarding the cobalt substituted phases, either a mixture of βIII- and γIII-type phases or a pure γIII-type [Co-8%(γ)] phase is obtained, depending on the amount of cobalt. During the oxidation of the chromium containing samples, the solution took a green colour, indicating a migration of chromium containing species towards the solution. This observation is not surprising since this element is well-known to dissolve easily in basic medium [21]. EDXS analyses are consistent with this result since no trace of chromium was found in the product of oxidizing Cr-substituted α-type phases. Finally, in the case of cadmium-substituted phase, the oxidized sample ended up as being a mixture of γ-type nickel oxihydroxide and β-type cadmium hydroxide (73-0969 *JCPDS* file) indicating that segregation of cadmium had taken place during oxidation.

In these last two examples (i.e. chromium or cadmium syntheses), the cell parameter of the γIII-phase obtained is exactly the same as the one of pure γIII-NiOOH phase (d_{003} = 7.03 Å), supporting the dissolution and segregation mechanisms, respectively. For the other samples, some small changes in the interlayer distance parameter are sometimes observed. The main difference appears for the Zn-37%(γ) sample which presents an interlayer distance of 7.49 Å. This larger cell parameter could be due to the presence of traces of αII within the sample.

Representative SEM images of substituted γIII-type oxidized phases are depicted in Fig. 9. For cobalt and zinc containing phases, some spheres presenting quite irregular forms and composed of agglomerates of thin tangled particles are observed and thus the texture of the corresponding α-type precursor is kept. In the cases of aluminium and iron substituted phases, the morphologies are not so well defined as in the corresponding precursors. Finally, in the case of cadmium-substituted samples, two types of particles with different morphology are observed within the same sample in agreement with the segregation of nickel and cadmium containing phases during the oxidation process.

3.4. Electrochemical tests of substituted γ-type nickel oxy-hydroxides in Ni/Zn cells

All the prepared samples were electrochemically tested, therefore for reasons of length and conciseness, we will only report the data obtained for samples (Table 1) as being almost pure γ-type phases (as deduced by XRD), and having a degree

Table 1
Average oxidation degree of nickel and experimental percentages of the substituting metal determined within both some selected γ-type phases and the corresponding substituted α-type precursors

M	M-substituted α-Ni(OH)$_2$		M-substituted γ-NiOOH	
	M-*x*%(sol)	M-*x*%(α)	M-*x*%(γ)	Average oxidation degree of Ni (±0.05)
Al	2.5	8	3.5	3.25
Cd	15	6	6	3.25
Co	2.5	8	8	3.35
Cr	2.5	8	0	3.20
Fe	2.5	7	7	3.30
Zn	1	4	4	3.35

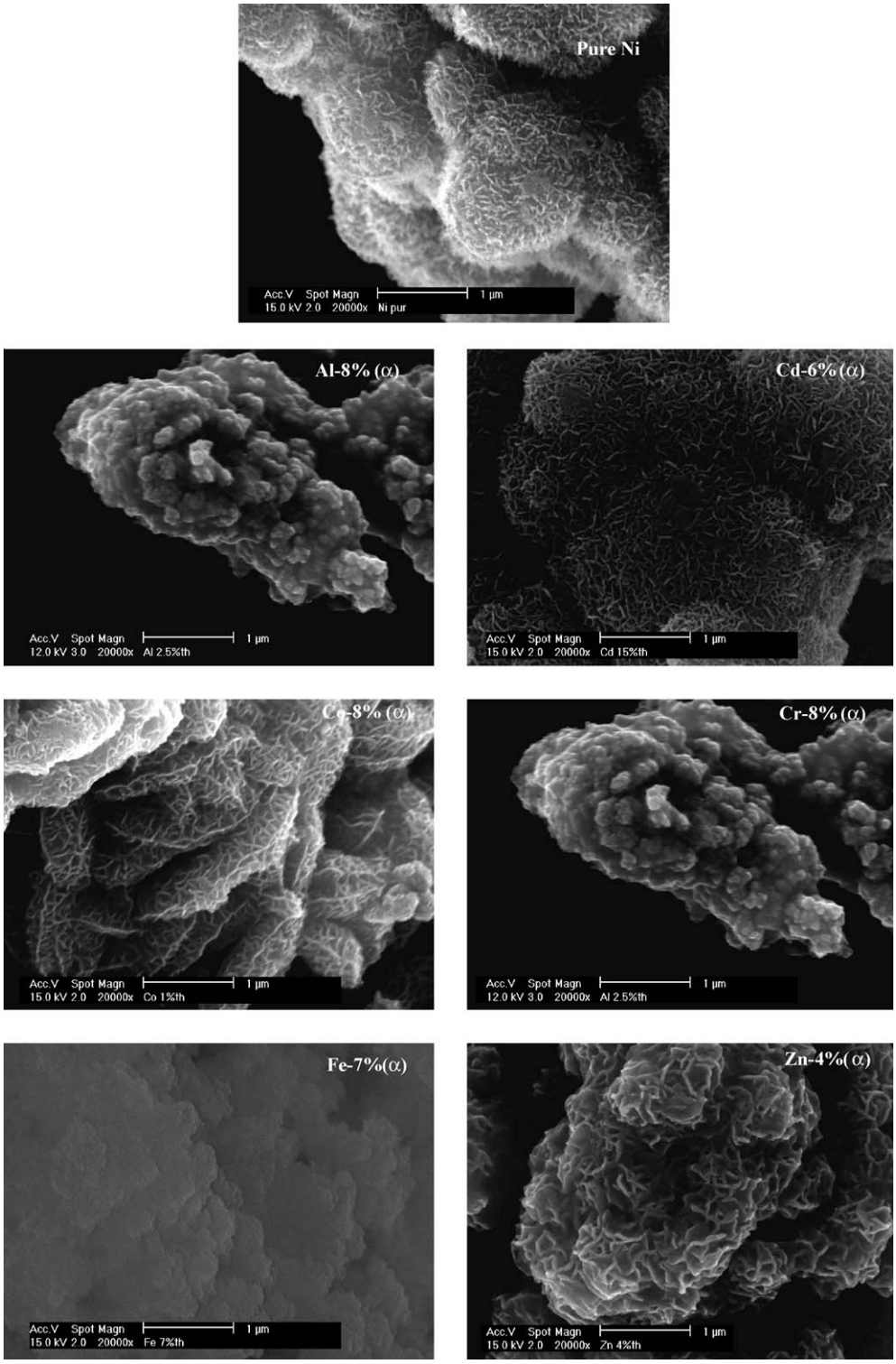

Fig. 7. SEM images of pure αII-Ni(OH)$_2$ and of M-substituted α-type nickel phases (with M = Al, Cd, Co, Cr, Fe or Zn). The percent of metal, *x*, present in the samples as determined by EDXS (M-*x*%(α)) are indicated. Pure nickel hydroxide texture, composed of aggregates of very thin tangled films is also observed in cobalt, cadmium or zinc substituted samples.

of substitution lower than 10%, which is the highest substituted values achieved in industrial β-type nickel hydroxides. The average oxidation degree of Ni within the Al-3.5%(γ), Cd-6%(γ), Co-8%(γ), Cr-0%(γ), Fe-7%(α) and Zn-4%(γ) phases (as determined by chemical titration) was found to range (Table 1) between 3.20 and 3.35 (±0.05), values relatively low for γ-type phase.

The samples were electrochemically tested as primary electrode materials in Ni/Zn primary button cells. For each sample composition eight cells were prepared. Four of them were

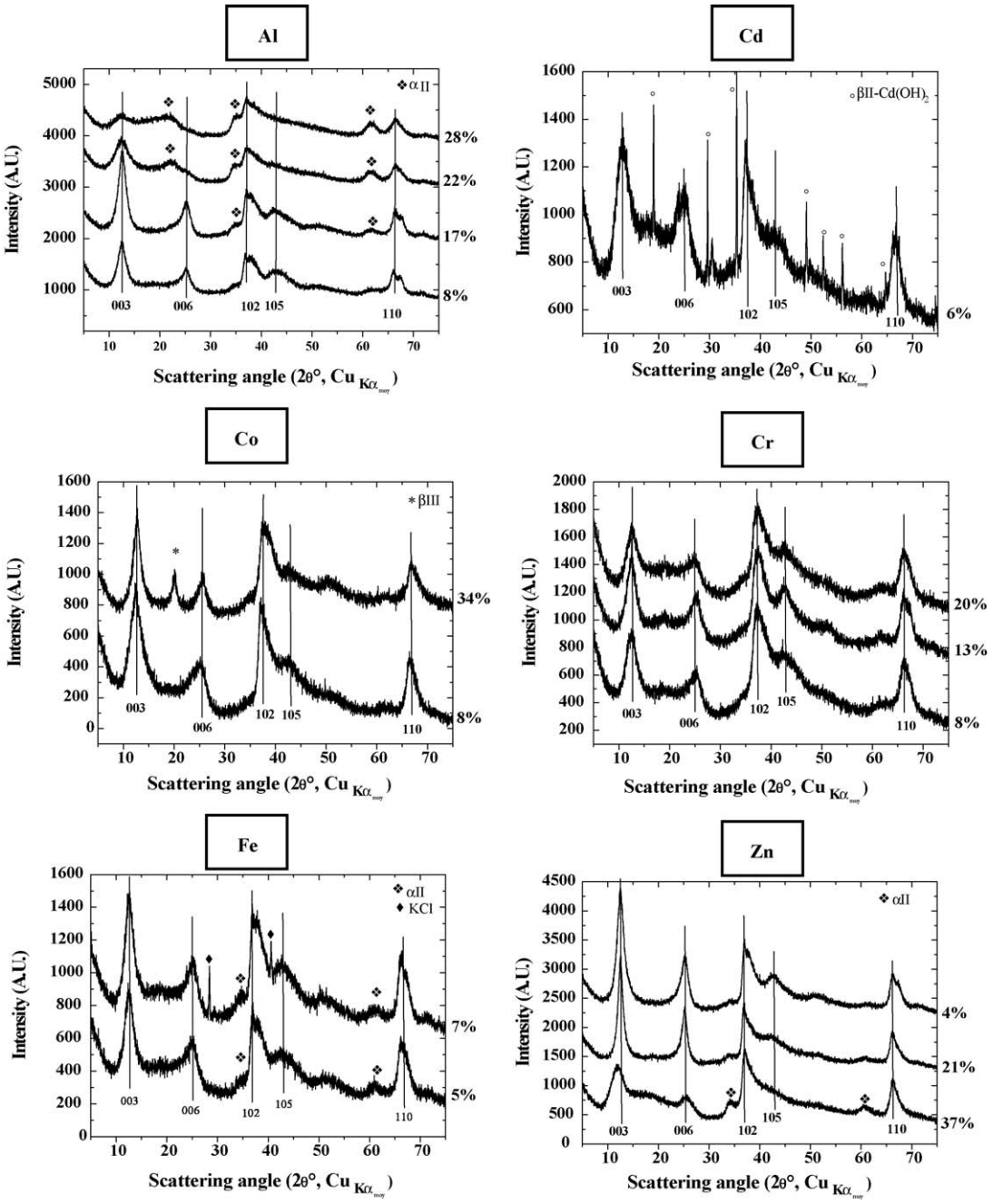

Fig. 8. X-ray diffraction patterns of M-substituted γ-type oxihydroxides prepared by oxidation of the substituted α-type nickel hydroxide precursors. Experimental percents, *x*, of M (M = Al, Cd, Co, Cr, Fe or Zn) determined by EDXS in final oxidized phases, denoted M-*x*%(γ), are indicated. Impurities (either α phase precursor, KCl from the reaction medium, $Cd(OH)_2$ or βIII) are indicated.

immediately discharged as soon they were assembled, and the remaining four were discharged after ageing of the button cell at 60 °C for 24 h. The resulting plots of voltage *U*(V) versus Zn/ZnO as a function of number of electron exchanged per unit formulae (NEE) are shown on Fig. 10. Owing to the constancy of the measured capacities to ±5% we have only reported for each sample composition one discharge for a fresh cell (solid line) and two for aged cells (dashed line). Pure γIII-NiOOH exchanges 0.42 electrons and loses 75% of its capacity after 24 h storage at 60 °C indicating that self-discharge is indeed a severe handicap for the application of these materials in primary batteries. Phases containing zinc or cadmium do not present any capacity. For the Zn-doped sample, the absence of capacity could be related to the fact that zinc species are probably situated in the interlayer space [13]. Regarding Cd-containing sample, the presence of βII-$Cd(OH)_2$, which pollutes the cathode material, is probably at the origin of its electrochemical inactivity. The phases substituted with aluminium, cobalt and iron present the best fresh capacities with approximately 0.52, 0.60 and 0.53 electrons exchanged, respectively. The fact that the number of electrons exchanged per formula unit is so low compared with the starting oxidation degree of nickel is certainly

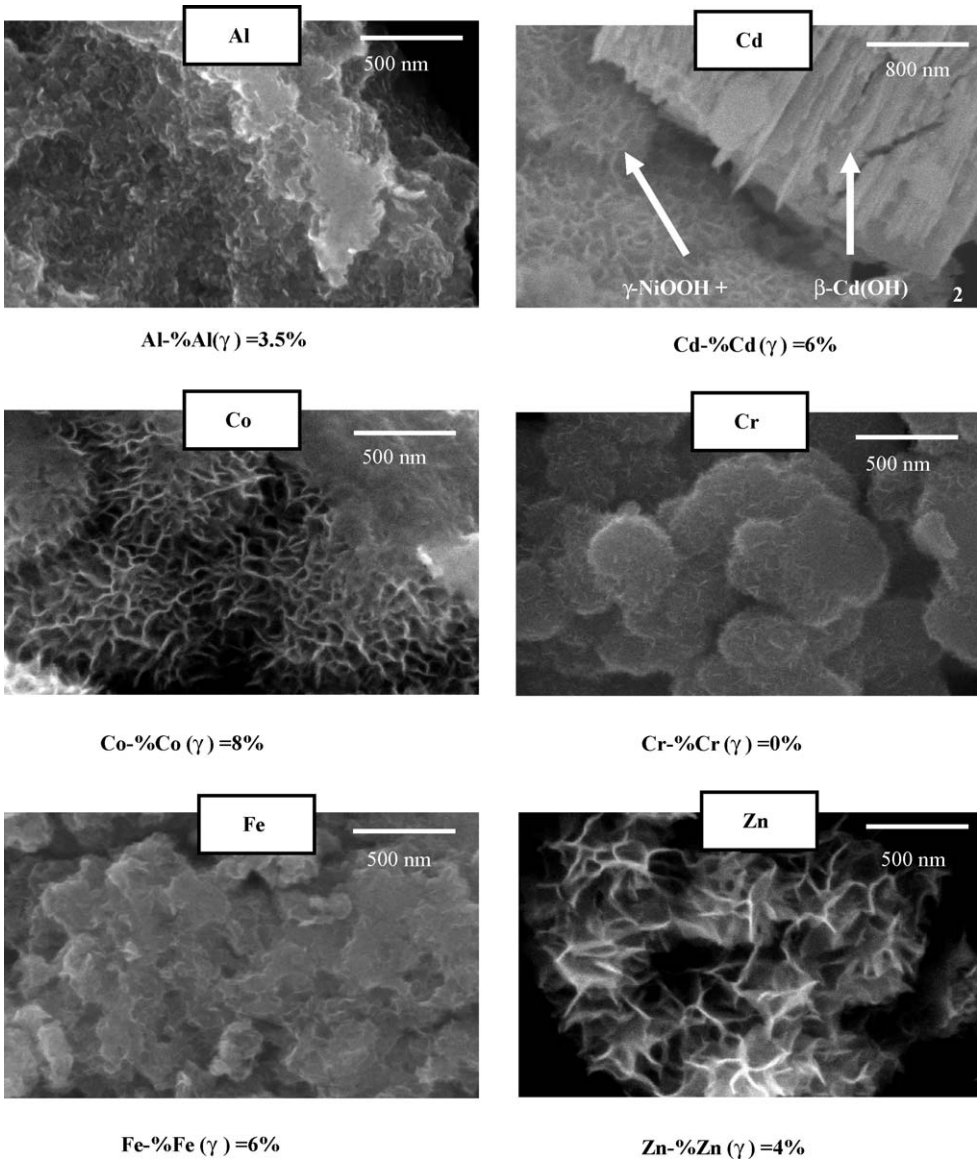

Fig. 9. Typical SEM images of M-substituted γ-type oxihydroxides. Experimental percents, *x*, of M (M = Al, Cd, Co, Cr, Fe or Zn) determined by EDXS in final oxidized phases, denoted M-*x*%M(γ), are indicated. For M = Co and Zn the texture of the corresponding α-type precursor are conserved whereas for M = Al or Fe, the morphologies are not so well defined, as in the corresponding precursors. For M = Cd, two morphologies are observed, corresponding to $Cd(OH)_2$ and γ-NiOOH segregated phases.

due to technological problems, as probably the morphology of the particles is not suitable to ensure a total contact with the carbon used as conducting additive in the electrode active material. Such a hypothesis was confirmed by an industrial survey of numerous electrodes composites containing different types of carbons together with γIII-phases powders of various morphologies, since composites having greater NEE could be achieved.

Regarding self-discharge performances, it is important to note that the discharge capacity of a Co- or Fe-based γIII/Zn phase is unaltered whether the cell was freshly discharged once made or discharged after being stored at 60 °C for 24 h. This is in contrast with the data for the Al-based Ni/Zn cells that show a drastic decrease in capacity between the fresh and aged cells. In the case of cobalt, it can be argued that this beneficial effect is due to the fact that cobalt substitution diminishes the Ni(III)/Ni(II) half discharge potential [27,28]. However, this does not apply in the case of substitution of nickel for iron, which is known to have the opposite effect and increase the Ni(III)/Ni(II) half-discharge potential [29,30]. The most probable explanation to the beneficial effect of cobalt or iron observed against self-discharge could lie in the fact that both cobalt and iron are well known to stabilize the αII-phase, which we believe to be an intermediate phase in the reduction, and this stabilization would considerably slow the self-discharge reaction. We can thus assume that self-discharge is initiated at the grains surface with the formation of a reduced αII layer, the solubility of which would control the kinetics of self-discharge. If it does not dissolve appreciably (as it would be the case for cobalt or iron substituted samples), it would play the role of a passivation layer preventing self-discharge.

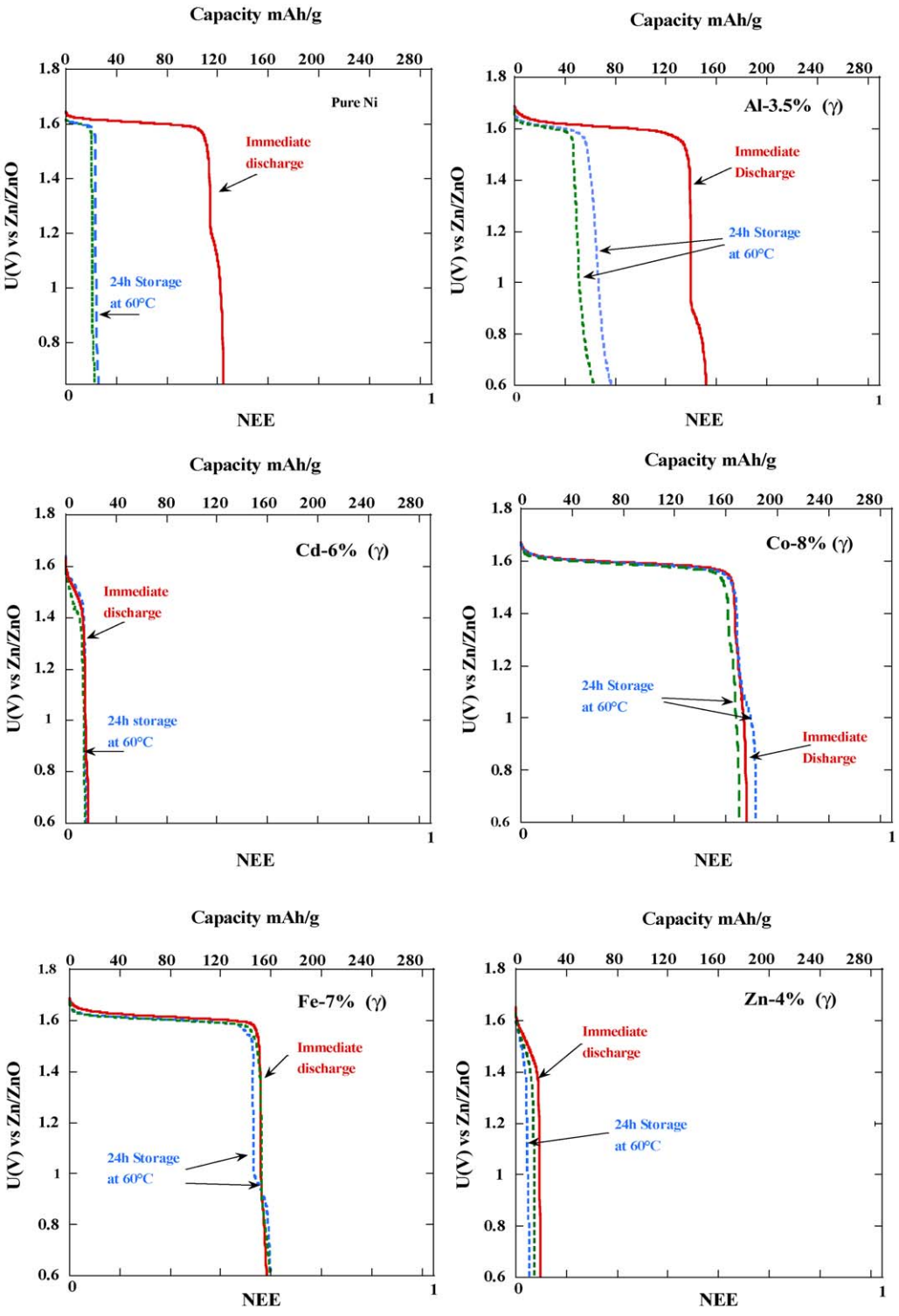

Fig. 10. Representative electrochemical first discharges of M-substituted γ-type oxihydroxide when used as positive electrode in Ni/Zn alkaline primary button cells. The potential vs. Zn/ZnO is represented as a function of the number of electrons exchanged (NEE) per formula unit. Solid line curves correspond to immediate discharges while dashed ones correspond to cells aged at 60 °C for 24 h. Except for cobalt and iron substituted samples, high temperature induces an important degree of self-discharge and almost no capacity is recovered.

4. Conclusion

The self-discharge of γ-NiOOH was studied both in real Ni/Zn primary cells and chemically simulated ones, and was found to consist of a dissolution/recrystallization process, certainly involving the presence of a α-type phase intermediate. With the aim of stabilizing this intermediate and therefore preventing self-discharge, metal substituted γ-type nickel hydroxide were prepared by oxidation in aqueous medium of α-type precursors synthesized at room temperature in an

ammonia containing medium. The amount of substituting metal in the α-type phases was higher than that present in the mother solution except in the case of cadmium. On the other hand, during the oxidation process this amount was maintained for cobalt, iron and zinc. Partial and total dissolution were observed for aluminium and chromium, whereas segregation of phases took place in the case of cadmium, respectively. Electrochemical tests performed on primary alkaline Ni/Zn button cells both as prepared and after 24 h storage at 60 °C indicate that iron and cobalt substitution are effective in preventing self-discharge in γ-type phases via the formation of a α-type phase which acts as a passivation layer. Such findings were king in paving the way towards the realization of practical Ni/Zn primary cells as will be reported at a later stage.

Acknowledgments

The authors would like to thank F. Sauvage, A. Delahaye-Vidal and P. Poizot for enlightening discussions. We are also indebted to Gillette Company for its financial support.

References

[1] S.A. Megahed, P.J. Spellman, Proceedings of the Symposium on Battery Devices, ECS Proceedings Series, vol. 79-1, 1979, p. 259.
[2] N. Sac-Epée, B. Beaudoin, V. Pralong, T. Jamin, J.-M. Tarascon, A. Delahaye-Vidal, J. Electrochem. Soc. 146 (7) (1999) 2376.
[3] V. Pralong, N. Sac-Epée, S. Taunier, B. Beaudoin, T. Jamin, A. Delahaye-Vidal, J.-M. Tarascon, J. Electrochem. Soc. 146 (7) (1999) 2382.
[4] N. Sac-Epée, Thèse de doctorat d'état, Amiens, 1997.
[5] H. Bode, K. Dehmelt, J. Witte, Electrochim. Acta 11 (1966) 1079.
[6] S. Le Bihan, M. Figlarz, C.R. Acad. Sci. 270 (1970) 2131.
[7] H. Bartl, H. Bode, G. Sterr, J. Witte, Electrochim. Acta 16 (1971) 615.
[8] A. Delahaye-Vidal, M. Figlarz, J. Appl. Electrochem. 17 (1987) 589.
[9] C. Faure, C. Delmas, J. Power Sources 35 (1991) 263.
[10] K. Tekaia-Ehlsissen, A. Delahaye-Vidal, P. Genin, M. Figlarz, P. Willmann, J. Mater. Chem. 3 (8) (1993) 883.
[11] C. Tessier, L. Guerlou-Demourgues, C. Faure, A. Demourgues, C. Delmas, J. Mater. Chem. 10 (2000) 1185.
[12] C. Tessier, L. Guerlou-Demourgues, C. Faure, M. Basterreix, G. Nabias, C. Delmas, J. Power Sources 133 (2000) 11.
[13] C. Lambert-Tessier, Thèse de doctorat d'état, Bordeaux, 1999.
[14] L. Guerlou-Demourgues, Thèse de doctorat d'état, Bordeaux, 1992.
[15] L. Guerlou-Demourgues, C. Denage, C. Delmas, J. Power Sources 52 (1994) 269.
[16] L. Guerlou-Demourgues, C. Denage, C. Delmas, J. Power Sources 52 (1994) 275.
[17] M. Dixit, P. Vishnu Kamath, J. Gopalakrishan, J. Electrochem. Soc. 146 (1) (1999) 79.
[18] J.J. Braconnier, Thèse de doctorat d'état, Bordeaux, 1983.
[19] Y. Borthomieu, Thèse de doctorat d'état, Bordeaux, 1990.
[20] M. Balasubramanian, C.A. Melendres, Electrochem. Solid State Lett. 2 (4) (1999) 167.
[21] R.S. Jayashree, P. Vishnu Kamath, J. Power Sources 107 (2002) 120.
[22] J. Besson, Ann. Chim. Ser. 2 2 (1947) 527–598.
[23] N. Sac-Epée, M.R. Palacín, A. Delahaye-Vidal, Y. Chabre, J.-M. Tarascon, J. Electrochem. Soc. 145 (5) (1998) 1434.
[24] R.D. Shannon, Acta Cryst. A 32 (1976) 751.
[25] J.-P. Jolivet, De la Solution à l'oxyde, Intereditions/CNRS Éditions, Paris, 1994.
[26] David R. Lide (Ed.), Handbook of Chemistry and Physics, 78th ed., CRC Press, 1997.
[27] C. Faure, C. Delmas, P. Willmann, J. Power Sources 36 (1991) 497.
[28] R.D. Armstrong, C.W.D. Briggs, E.A. Charles, J. Appl. Electrochem. 18 (1988) 215.
[29] O. Glemser, D.H. Buss, J. Bauer, H. Low, Patent number DE3811717-A, 1988.
[30] L. Guerlou-Demougues, C. Delmas, J. Electrochem. Soc. 141 (1994) 713.